IOP FTC
IOP Publishing
Journal of Physics: Condensed Matter
J. Phys.: Condens. Matter **22** (2010) 292202 (5pp)
doi:10.1088/0953-8984/22/29/292202

FAST TRACK COMMUNICATION

Anomalous compressibility effects and superconductivity of $EuFe_2As_2$ under high pressures

Walter Uhoya[1], Georgiy Tsoi[1], Yogesh K Vohra[1], Michael A McGuire[2], Athena S Sefat[2], Brian C Sales[2], David Mandrus[2] and Samuel T Weir[3]

[1] Department of Physics, University of Alabama at Birmingham (UAB), Birmingham, AL 35294, USA
[2] Oak Ridge National Laboratory (ORNL), Oak Ridge, TN 37831, USA
[3] Mail Stop L-041, Lawrence Livermore National Laboratory (LLNL), Livermore, CA 94550, USA

Received 5 May 2010, in final form 15 May 2010
Published 29 June 2010
Online at stacks.iop.org/JPhysCM/22/292202

Abstract
The crystal structure and electrical resistance of structurally layered $EuFe_2As_2$ have been studied up to 70 GPa and down to a temperature of 10 K, using a synchrotron x-ray source and designer diamond anvils. The room temperature compression of the tetragonal phase of $EuFe_2As_2$ ($I4/mmm$) results in an increase in the a-axis length and a rapid decrease in the c-axis length with increasing pressure. This anomalous compression reaches a maximum at 8 GPa and the tetragonal lattice behaves normally above 10 GPa, with a nearly constant c/a axial ratio. The rapid rise in the superconducting transition temperature (T_c) to 41 K with increasing pressure is correlated with this anomalous compression, and a decrease in T_c is observed above 10 GPa. We present P–V data or the equation of state for $EuFe_2As_2$ both in the ambient tetragonal phase and in the high pressure collapsed tetragonal phase up to 70 GPa.

The discovery of a new class of iron arsenide superconductors [1] has provided fresh impetus to high pressure studies on these materials where the pressure variable provides a controlled tuning of the superconducting properties without the disorder effects induced by chemical substitution or doping. The so called 122 iron-based superconducting materials AFe_2As_2 (A = divalent alkaline earth or rare earth metal Ca, Sr, Ba, and Eu) are of particular interest because of the overlap of the superconducting and antiferromagnetic phases in these materials. In particular, the 122 compound $EuFe_2As_2$ has been investigated to only modest pressures of 3 GPa and pressure-induced superconductivity has been reported beginning at approximately 2 GPa [2, 3]. The high pressure studies on $EuFe_2As_2$ are intriguing because a simultaneous occurrence of superconductivity and antiferromagnetic ordering is observed at high pressures and low temperatures [2, 3]. The structural and magnetic phase transitions have been extensively investigated at ambient pressure and at low temperatures for $EuFe_2As_2$ [4, 5] and reveal two phase transitions at 190 K and 20 K respectively. The phase transition at $T_0 = 190$ K at ambient pressure is attributed to a spin density wave (SDW) and results in a crystallographic phase transition from the ambient tetragonal phase ($I4/mmm$) to an orthorhombic phase ($Fmmm$), and the Fe moments order antiferromagnetically. The phase transition at 20 K is an antiferromagnetic ordering of the Eu^{2+} moments and the temperature at which it occurs is referred to as the Néel temperature (T_N). The SDW transition is suppressed by the application of high pressure, and the transition temperature T_0 is found to decrease rapidly with increasing pressure; the SDW transition is not detected above 2.5 GPa. The previous high pressure studies on $EuFe_2As_2$ indicate that T_N is relatively insensitive to pressure and remains at 20 K up to 3 GPa, while the superconductivity transition temperature T_c appears at 30 K at a pressure of 2.8 GPa [2, 3].

The present study is motivated by the occurrence of superconductivity under high pressure in $EuFe_2As_2$ and its

correlation with the compression of the tetragonal (T) lattice and the possible occurrence of a collapsed tetragonal (CT) phase under high pressures. The compression behavior of $BaFe_2As_2$ has been studied up to 22 GPa at ambient temperature and anisotropic compression effects have been documented [6]. The first-order and second-order phase transitions of ternary europium phosphides with $ThCr_2Si_2$-type structure have been reported under high pressure [7]. Also, a nonmagnetic CT phase has been documented in $CaFe_2As_2$ at $P = 0.24$ GPa and $T = 50$ K [8], and the impact of the CT phase on the superconducting properties of $CaFe_2As_s$ has been extensively studied [9–11]. An additional consideration for present studies is that the high pressure Mössbauer investigations on $EuFe_2P_2$ have revealed a continuous valence transition from a magnetic Eu^{2+} state to a nonmagnetic Eu^{3+} state in the pressure range between 3 and 9 GPa [12]. We have carried out detailed structural studies on $EuFe_2As_2$ under ultrahigh pressures to 70 GPa at ambient temperature using image plate x-ray diffraction at a synchrotron source.

The single-crystal samples of $EuFe_2As_2$ were grown using FeAs self-flux methods as described in [13]. The single-crystal sample was powdered and loaded in a diamond anvil cell for high pressure x-ray diffraction experiments. Our x-ray diffraction studies at ambient pressure and temperature revealed a tetragonal structure with lattice parameters $a = 3.916 \pm 0.012$ Å and $c = 12.052 \pm 0.036$ Å with axial ratio $c/a = 3.078$ at ambient temperature and pressure. The tetragonal crystal structure of $EuFe_2As_2$ is identified as of $ThCr_2Si_2$ type with space group $I4/mmm$, with Eu atoms at the 2a position (0, 0, 0), Fe atoms at 4d positions (0, 1/2, 1/4) and (1/2, 0, 1/4), and As atoms at 4e positions $(0, 0, z)$ and $(0, 0, -z)$. The structural parameter $z = 0.3625$ has been obtained from Rietveld refinement of x-ray diffraction data [4]. The high pressure x-ray diffraction experiments were carried out at the beam-line 16-ID-B, HPCAT, Advanced Photon Source, Argonne National Laboratory. An angle dispersive technique with an image plate area detector was employed using an x-ray wavelength $\lambda = 0.4072$ Å. We employed eight-probe designer diamond anvils [14, 15] in high pressure four-probe electrical resistance measurements on the $EuFe_2As_2$ compound. The eight tungsten microprobes are encapsulated in a homoepitaxial diamond film and are exposed only near the tip of the diamond to make contact with the $EuFe_2As_2$ sample at high pressure. Two electrical leads are used to set constant current through the sample and the two additional leads are used to monitor the voltage across the sample. The pressure was monitored by the ruby fluorescence technique and care was taken to carefully calibrate the ruby R_1 emission to the low temperature of 10 K as described in an earlier publication [16]. In x-ray diffraction experiments, an internal copper pressure standard was employed for the calibration of the pressure [17]. The Birch–Murnaghan equation [18], shown as equation (1), was fitted to the available equation of state data on a copper pressure standard [17]:

$$P = 3B_0 f_E (1 + 2f_E)^{5/2} \left\{1 + \tfrac{3}{2}(B' - 4) f_E\right\} \qquad (1)$$

where B_0 is the bulk modulus, B' is the first derivative of the bulk modulus at ambient pressure, and V_0 is the ambient

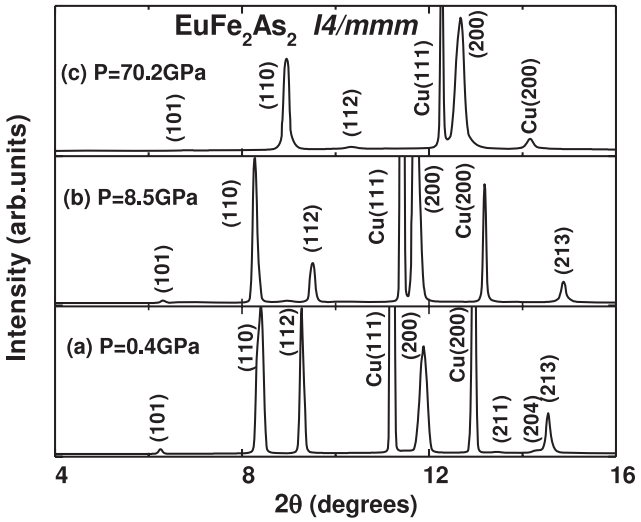

Figure 1. The integrated x-ray diffraction profiles for $EuFe_2As_2$ at various pressures at ambient temperature obtained using an x-ray wavelength $\lambda = 0.4072$ Å. (a) Diffraction pattern at a low pressure of 0.4 GPa. (b) Diffraction pattern at 8.5 GPa showing anomalous compression effects discussed in the text. (c) Diffraction pattern at the highest pressure of 70.2 GPa showing stability of the tetragonal phase. The copper (Cu) pressure marker diffraction peaks are present in all spectra.

pressure volume. The fitted values for the copper pressure standard are $B_0 = 121.6$ GPa, $B' = 5.583$, and $V_0 = 11.802$ Å^3/atom.

The parameter f_E is related to the volume compression and is described below:

$$f_E = \frac{\left[\left(\frac{V_0}{V}\right)^{2/3} - 1\right]}{2}. \qquad (2)$$

Figure 1 shows the integrated x-ray diffraction profiles for $EuFe_2As_2$ obtained at various pressures from the image plate diffraction studies at the beam-line 16-ID-B, Advanced Photon Source, Argonne National Laboratory, using a wavelength $\lambda = 0.4072$ Å. The image plate x-ray diffraction patterns were recorded with a 5 μm × 5 μm x-ray beam focused on an 80 μm diameter $EuFe_2As_2$ sample mixed with copper pressure marker. The use of a focused x-ray beam allows us to collect high quality x-ray diffraction patterns that are not affected by the inhomogeneous pressure conditions of the sample. The geometrical constraints in our diamond anvil cell device allowed x-ray diffraction data to be obtained to 2θ below 15° (or interplanar d-spacing > 1.56 Å). Figure 1(a) shows the x-ray diffraction pattern at 0.4 GPa with the $EuFe_2As_2$ sample in the $I4/mmm$ tetragonal phase and the copper pressure marker in the face centered cubic (fcc) phase. The diffraction peaks are labeled with their respective (hkl) values. The tetragonal phase of $EuFe_2As_2$ is characterized by the (101), (110), (112), (200), (211), (204), and (213) diffraction peaks. The fcc phase of the copper pressure marker is characterized by the (111) and (200) diffraction peaks. The measured volume of copper obtained from the x-ray diffraction was used to calculate the sample pressure from the equation of state given by equation (1). The measured lattice parameters at 0.4 GPa are $a = 3.923 \pm$

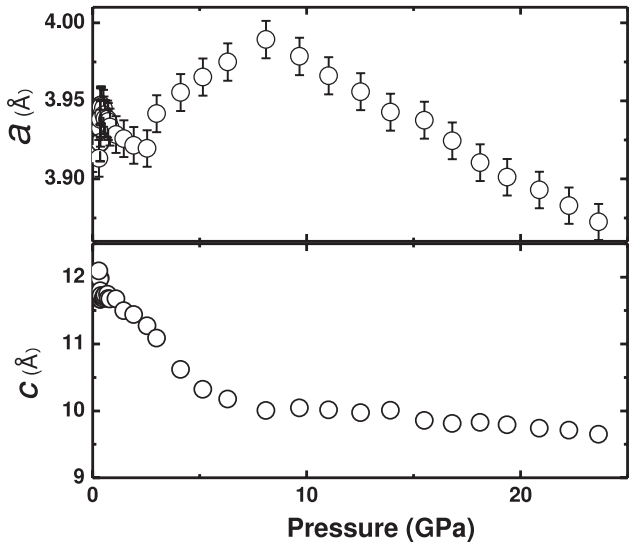

Figure 2. The measured lattice parameters a and c for the tetragonal phase of $EuFe_2As_2$ as a function of pressure. A negative compressibility is observed for the a-axis and a maximum is observed at 8.5 GPa. The c-axis shows a rapid decrease with increasing pressure up to 8 GPa and a normal decrease with further increase in pressure. The error bars for c are less than the symbol size used in plotting.

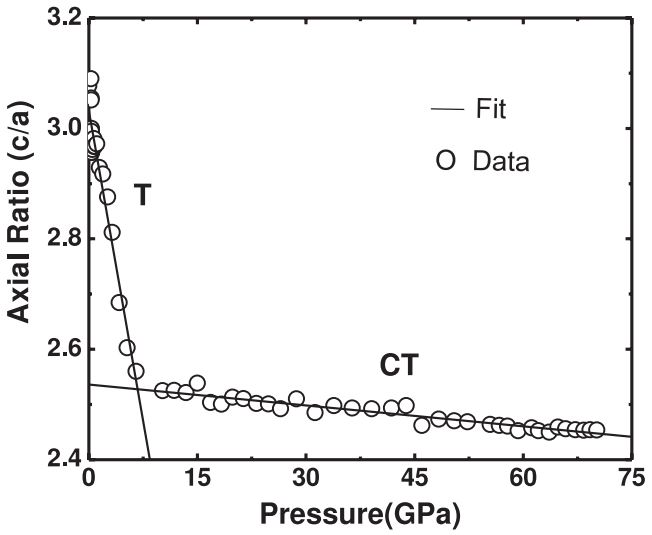

Figure 3. The measured axial ratio (c/a) for the tetragonal phase of $EuFe_2As_2$ as a function of pressure up to 70 GPa. The linear fits for the two phases, i.e., the tetragonal (T) phase and the collapsed tetragonal (CT) phase, are described in the text. The transition between the two phases occurs at 8 GPa at ambient temperature.

0.012 Å and $c = 11.985 \pm 0.036$ Å. Figure 1(b) shows the x-ray diffraction spectrum at a pressure of 8.5 GPa with lattice parameters $a = 3.989 \pm 0.012$ Å and $c = 10.006 \pm 0.030$ Å. The $EuFe_2As_2$ (101), (112), and (213) diffraction peaks clearly show a movement to higher diffraction angles or lower interplanar spacing with increasing pressure while the (110) and (200) ones move to lower diffraction angles or higher interplanar spacing when comparing x-ray diffraction patterns at 8.5–0.4 GPa (figures 1(a) and (b)). This is clear evidence of the anomalous compression of the tetragonal lattice as the a-axis length increases with increasing pressure and the c-axis length decreases with increasing pressure. This is in contrast to normal compression behavior which shows a uniform decrease in all dimensions of the unit cell. Another important point to note is that the $EuFe_2As_2$ (213) diffraction peak remains a single peak without any evidence of splitting and hence there is no evidence of a tetragonal to orthorhombic phase transformation at high pressures as has been noted at low temperatures [4, 5]. Figure 1(c) shows that the phase remains tetragonal up to the highest pressure of 70.2 GPa with lattice parameters $a = 3.692 \pm 0.011$ Å and $c = 9.059 \pm 0.027$ Å. The compression of the tetragonal lattice between 8.5 and 70.2 GPa can be considered normal, as all diffraction peaks move to higher angles or lower interplanar d-spacings as can be seen by comparing figures 1(b) and (c).

Figure 2 shows the measured lattice parameters a and c as a function of pressure, exhibiting anomalous compression effects. The lattice parameter a shows an initial decrease with pressure of 2.6 GPa followed by an increase with increasing pressure with a peak at a pressure of 8.5 GPa. A further increase in pressure beyond 8 GPa results in a decrease in a and a normal compression behavior that continues up to the highest pressure of 70 GPa. This negative compressibility of the a lattice parameter is a very intriguing feature of $EuFe_2As_2$ compression. The lattice parameter c shows a rapid decrease with increasing pressure up to 8 GPa and a normal decrease with further increase in pressure up to 70 GPa.

Figure 3 shows the measured axial ratio (c/a) as a function of pressure up to 70 GPa at ambient temperature. The axial ratio (c/a) shows a rapid decrease with increasing pressure up to 8 GPa and a gradual decrease above this pressure. In fact, the c/a ratio variation as a function of pressure can be divided into two linear regions and the fits for the two linear regions are shown in figure 3 and described below:

$$c/a = 3.033 - 0.075P, \qquad 0 \leqslant P \leqslant 8 \text{ GPa}, \tag{3}$$

$$c/a = 2.536 - 0.001P, \qquad 10 \leqslant P \leqslant 70 \text{ GPa}. \tag{4}$$

The intersection of the two linear regions as described by equations (3) and (4) defines the phase transition from the ambient pressure T phase to the so called CT phase. This phase transition is defined by the present experiments to occur near 8 GPa at ambient temperature. A further x-ray diffraction study at low temperature would be needed to follow this phase boundary to low temperatures.

Figure 4 shows the measured pressure–volume (P–V) curve or equation of state for $EuFe_2As_2$ up to 70 GPa at ambient temperature. Also shown are the Birch–Murnaghan equation of state fits as described by equation (1). The fit parameters for the tetragonal and collapsed tetragonal phases are summarized in table 1. The fitted ambient pressure volume (V_0) is 184.5 Å^3 for the T phase and is 170.0 Å^3 for the CT phase, indicating that a hypothetical CT phase at ambient pressure has a density that is 7.9% higher than the T phase one (table 1). The measured equation of state shows considerable stiffening at the tetragonal to collapsed tetragonal

Table 1. Equation of state parameters for the $EuFe_2As_2$ sample in the tetragonal (T) phase and collapsed tetragonal (CT) phase at ambient temperature.

Phase	Unit cell volume (V_0) ambient conditions	Bulk modulus (B_0)	Pressure derivative of bulk modulus (B')
Tetragonal (T) $0 < P < 8$ GPa	184.5 ± 0.4 Å^3	39.3 ± 1.6 GPa	6.9 ± 0.4
Collapsed tetragonal (CT) 10 GPa $< P <$ 70 GPa	170.0 ± 0.4 Å^3	134.0 ± 1.6 GPa	3.3 ± 0.2

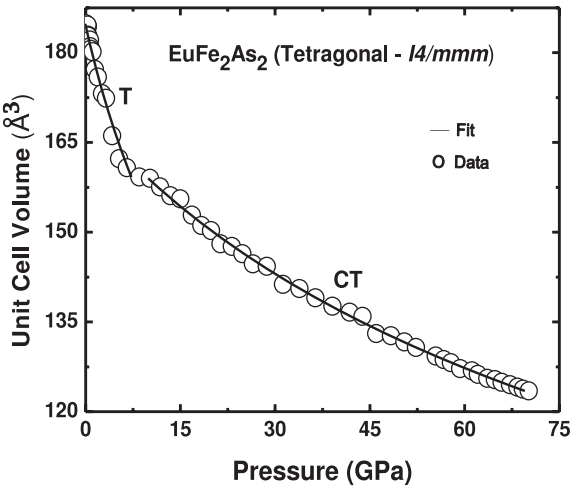

Figure 4. The measured equation of state data for the tetragonal phase of $EuFe_2As_2$ as a function of pressure up to 70 GPa. The solid curves are the Birch–Murnaghan equation of state fit to the two phases, i.e., the tetragonal (T) phase and the collapsed tetragonal (CT) phase. The fit parameters are summarized in table 1. The transition between the two phases occurs at 8 GPa at ambient temperature.

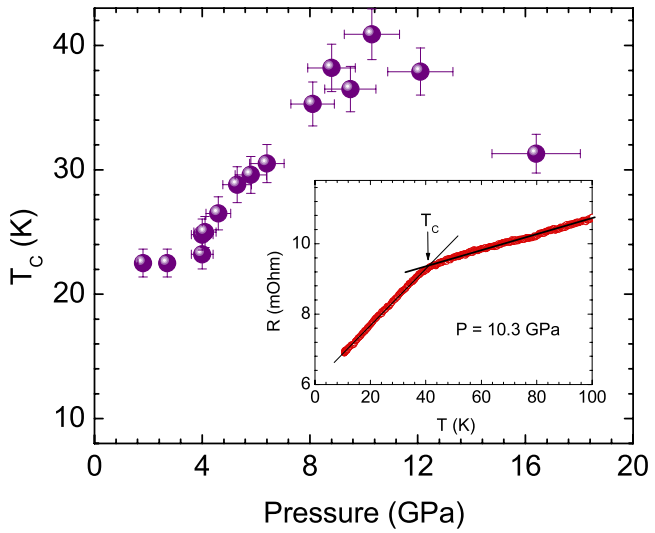

Figure 5. The measured superconducting transition (T_c) temperature as a function of pressure for $EuFe_2As_2$ as obtained from electrical resistivity measurements. T_c shows an increase between 4 GPa and 10 GPa and gets to as high as 41 K. The T_c shows a gradual decrease above 10 GPa and correlates with the anomalous compressibility effects in this material. The inset shows electrical resistance as a function of temperature at 10.3 GPa, indicating the onset of superconductivity at 41 K.

(This figure is in colour only in the electronic version)

phase transition, as evidenced by an abrupt change in slope of the volume–pressure curve at 8 GPa as shown in figure 4. The fitted value of the bulk modulus is $B_0 = 39.3$ GPa for the T phase and $B_0 = 134.0$ GPa for the CT phase at ambient pressure. This comparison shows that the T phase of $EuFe_2As_2$ is more compressible than a hypothetical CT phase at ambient pressure, by a factor of 3.4.

Figure 5 shows the measured superconducting transition temperature T_c as a function of pressure. The T_c measurements have been carried out using four-probe electrical resistance measurements using a designer diamond anvil as described in an earlier publication [16]. The inset in figure 5 shows electrical resistance as a function of temperature at a pressure of 10.3 GPa, indicating the temperature for the onset of superconductivity, T_c, to be 41 K. It is interesting to note that T_c shows a rapid increase in the pressure region where anomalous compression effects were observed in x-ray diffraction experiments. In particular, T_c shows a rapid increase between 4 and 10 GPa and attains a value as high as 41 K near 10 GPa. A further increase in pressure beyond 10 GPa leads to a reduction in T_c in the CT phase. It seems that anomalous compression tends to favor superconductivity as the FeAs tetrahedral bonded layers are brought together, and then it shows a decrease as we reach the compression limit of the tetragonal phase and as a collapsed tetragonal structure is formed. The structural distortions under pressure and chemical doping in superconducting $BaFe_2As_2$ and $CeFeAsO_{1-x}F_x$ have been correlated with the superconducting properties [19, 20]. In particular, the superconducting transition temperature T_c is found to increase for $BaFe_2As_2$ as the As–Fe–As bond angles tend to the ideal tetrahedral value of 109.5° [19]. Our measured lattice parameters $a = 3.989 \pm 0.012$ Å and $c = 10.006 \pm 0.030$ Å at 8.5 GPa for $EuFe_2As_2$, along with an estimated structural parameter $z = 0.370$, result in As–Fe–As bond angles of 105.5° and 117.7°. The structural parameter z is not well constrained in our experiments due to the limited diffraction data set and preferred alignment of crystal grains common in high pressure experiments. The estimated As–Fe–As bond angle values for $EuFe_2As_2$ are far removed from the ideal bond angles of 109.5° observed in $BaFe_2As_2$; however, it should be noted that $EuFe_2As_2$ is different from the other 122 superconducting materials due to a valence transition from a magnetic Eu^{2+} state to a nonmagnetic Eu^{3+} state that occurs in the pressure range between 3 and 9 GPa [12]. A complete description of the superconducting properties of $EuFe_2As_2$ would likely involve both the structural changes documented in

this paper and the valence transition recorded in high pressure Mössbauer investigations.

In summary, we have studied the 122 iron-based layered compound $EuFe_2As_2$ up to 70 GPa at ambient temperature using a synchrotron source. The image plate x-ray diffraction studies reveal anomalous compressibility effects where the a-axis length of the tetragonal phase shows an increase with increasing pressure while the c-axis length shows a rapid decrease with increasing pressure. A maximum in a-axis length is observed at a pressure of 8 GPa and a normal compression behavior is observed above this pressure. The phase above 8 GPa is referred to as the collapsed tetragonal (CT) phase, as opposed to the normal tetragonal (T) phase. The equations of state for the T phase and CT phase show distinct bulk moduli (B_0) and pressure derivatives of the bulk moduli (B'). At ambient pressure, an extrapolated CT phase has a density that is 7.9% higher as compared to the T phase under similar conditions. The superconductivity in $EuFe_2As_2$ has been studied under high pressure using four-probe electrical resistance measurements with designer diamond anvils. The superconductivity transition temperature (T_c) is marked by a decrease in electrical resistance as a function of temperature. The measured value of T_c shows an increase between 4 GPa and 10 GPa and attains a value as high as 41 K under high pressure. This increase in T_c is correlated with the anomalous compressibility effects documented in this report. The superconducting transition temperature T_c shows a gradual decrease with pressure above 10 GPa in the CT phase. Our high pressure studies on 122 iron-based layered superconductor $EuFe_2As_2$ have shown anomalous compressibility effects, the presence of a collapsed tetragonal phase, and superconducting properties that are strongly linked to its compression behavior.

Walter Uhoya acknowledges support from the Carnegie/Department of Energy (DOE) Alliance Center (CDAC) under Grant No. DE-FC52-08NA28554. Research at ORNL is sponsored by the Division of Materials Sciences and Engineering, Office of Basic Energy Sciences, US Department of Energy. Portions of this work were performed at HPCAT (Sector 16), Advanced Photon Source (APS), Argonne National Laboratory.

References

[1] Kamihara Y, Watanabe T, Hirano M and Hosono H 2008 *J. Am. Chem. Soc.* **130** 3296
[2] Miclea C F, Nicklas M, Jeevan H S, Kasinathan D, Hossain Z, Rosner H, Gegenwart P, Geibel C and Steglich F 2009 *Phys. Rev.* B **79** 212509
[3] Terashima T, Kimata M, Satsukawa H, Harada A, Hazama K, Uji S, Suzuki H, Matsumoto T and Murata K 2009 *J. Phys. Soc. Japan* **78** 083701
[4] Tegel M, Rotter M, Weiß V, Schappacher F M, Pöttgen R and Johrendt D 2008 *J. Phys.: Condens. Matter* **20** 452201
[5] Ren Z, Zhu Z, Jiang S, Xu X, Tao Q, Wang C, Feng C, Cao G and Xu Z 2008 *Phys. Rev.* B **78** 052501
[6] Jorgensen J-E, Staun Olsen J and Gerward L 2009 *Solid State Commun.* **149** 1161
[7] Huhnt C, Schlabitz W, Wurth A, Mewis A and Reehuis M 1998 *Physica* B **252** 44
[8] Kreyssig A, Green M A, Lee Y, Samolyuk G D, Zajdel P, Lynn J W, Bud'ko S L, Torikachvili M S, Ni N, Nandi S, Leao J, Poulton S J, Argyriou D N, Harmon B N, McQueeney R J, Canfield P C and Coldman A I 2008 *Phys. Rev.* B **78** 184517
[9] Torikachvili M S, Bud'ko S L, Ni N and Canfield P C 2008 *Phys. Rev. Lett.* **101** 057006
[10] Yu W, Aczel A A, Williams T J, Bud'ko S L, Ni N, Canfield P C and Luke G M 2009 *Phys. Rev.* B **79** 020511(R)
[11] Kawasaki S, Tabuchi T, Wang X F, Chen X H and Zheng G-Q 2010 *Supercond. Sci. Technol.* **23** 054004
[12] Ni B, Abd-Elmeguid M M, Micklitz H, Sanchez J P, Vulliet P and Johrendt D 2001 *Phys. Rev.* B **63** 100102(R)
[13] Sefat A S, Jin R, McGuire M A, Sales B C, Singh D J and Mandrus D 2008 *Phys. Rev. Lett.* **101** 117004
[14] Weir S T, Akella J, Ruddle C A, Vohra Y K and Catledge S A 2000 *Appl. Phys. Lett.* **77** 3400
[15] Vohra Y K and Weir S T 2002 High pressure phenomenon *Proc. Int. School of Physics—Enrico Fermi, Course XXLVII* ed R J Hemley, G L Chiarotti, M Bernasconi and L Ulivi (Bologna: IOS Press) p 87
[16] Tsoi G, Stemshorn A, Vohra Y K, Wu P M, Hsu F C, Huang Y L, Wu M K, Yeh K W and Weir S T 2009 High pressure superconductivity in iron based layered compounds studied using designer diamonds *J. Phys.: Condens. Matter* **21** 232201
[17] Velisavljevic N and Vohra Y K 2004 *High Pressure Res.* **24** 295
[18] Birch F 1947 *Phys. Rev.* **71** 809
[19] Kimber S A J, Kreyssig A, Zhang Y-Z, Jeschke H O, Valentí R, Yokaichiya F, Colombier E, Yan J, Hansen T C, Chatterji T, McQueeney R J, Canfield P C, Goldman A I and Argyriou D N 2009 *Nat. Mater.* **8** 471
[20] Zhao J, Huang Q, de la Cruz C, Li S, Lynn J W, Chen Y, Green M A, Chen G F, Li G, Li Z, Luo J L, Wang N L and Dai P 2008 *Nat. Mater.* **7** 953